Detecting slow magnetization relaxation via magnetotransport measurements based on the current-reversal method

Sebastian Beckert, Richard Schlitz, Gregor Skobjin, Antonin Badura, Miina Leiviskä, Dominik Kriegner, Daniel Scheffler, Giacomo Sala, Kamil Olejník, Lisa Michez, et al.

Editors' Suggestion

Detecting slow magnetization relaxation via magnetotransport measurements based on the current-reversal method

Sebastian Beckert,[1] Richard Schlitz,[2] Gregor Skobjin,[2] Antonin Badura,[3] Miina Leiviskä,[3,4] Dominik Kriegner,[1,3] Daniel Scheffler,[1,3] Giacomo Sala,[5] Nadine Nabben,[2] Xian-Yue Ai,[2] Kamil Olejník,[3] Lisa Michez,[6] Vincent Baltz,[4] Andy Thomas,[1,7] Helena Reichlová,[1,3] and Sebastian T. B. Goennenwein[2]

[1]*Institut für Festkörper- und Materialphysik, Technische Universität Dresden, 01062 Dresden, Germany*

[2]*Department of Physics, University of Konstanz, 78457 Konstanz, Germany*

[3]*Institute of Physics ASCR, v.v.i., Cukrovarnická 10, 162 53 Prague, Czech Republic*

[4]*Univ. Grenoble Alpes, CNRS, CEA, Grenoble INP, IRIG-Spintec, F-38000 Grenoble, France*

[5]*Department of Materials, ETH Zurich, CH-8093 Zurich, Switzerland*

[6]*Aix-Marseille Univ., CNRS, CINaM, Marseille, France*

[7]*Leibniz Institute of Solid State and Materials Science (IFW Dresden), Helmholtzstrasse 20, 01069 Dresden, Germany*

(Received 27 May 2024; accepted 7 January 2025; published 27 January 2025)

Slow magnetization relaxation processes are an important time-dependent property of many magnetic materials. We show that magnetotransport measurements based on a well-established current-reversal method can be utilized to implement a simple and robust screening scheme for such relaxation processes. We demonstrate our approach considering the anomalous Hall effect in a Pt/Co/AlO_x trilayer model system, and then explore relaxation in τ-MnAl films. Compared to magnetotransport experiments based on ac lock-in techniques, we find that the dc current-reversal method is particularly sensitive to relaxation processes which happen on timescales on the order of few to many seconds.

DOI: 10.1103/PhysRevB.111.014441

I. INTRODUCTION

Slow magnetization relaxation processes in magnetic materials, i.e., the delayed response of the magnetization to the external magnetic field [1], have been observed and investigated for several decades, as described by Néel [2], Preisach [1], and others [3–11]. Over time, slow relaxation processes have been reported in materials with various magnetic properties, including thin films with perpendicular magnetic anisotropy (PMA) [5,10,12,13], spin glasses [10], and compensated magnets [14,15]. Magnetic relaxation can be probed by the magneto-optical Kerr effect [5,7–9], magnetometry [4,12], magnetic microscopy [6,16], and the anomalous Hall effect (AHE) [11,17,18]. The relaxation processes also impact magnetic characterization experiments. For example, the coercive field measured in recording tape depends on the field sweep rate owing to relaxation effects [19]. Similar observations have also been reported in AHE experiments on thin films [18]. Indeed, the time necessary for the reversal of the magnetization to reach a new (quasi-)equilibrium state can vary over many orders of magnitude, depending on various parameters such as the material, sample size, defects, temperature, and external magnetic field strength. It can be quasi-instantaneous [20] or reach up to several hundreds or thousands of seconds [4,5]. Even in the same material system, the timescales of the relaxation can vary over several orders of magnitude, as has been shown for Au/Co/Au sandwiches by Bayreuther *et al.* [4]. In the following, we limit the considerations to slow magnetization relaxation, i.e., relaxation processes which happen on timescales ranging from a few seconds [5–7] up to thousands of seconds [5].

In-depth studies of slow magnetization relaxation processes require either the measurement of the time evolution of the magnetization over long time intervals, at fixed magnetic field, or a series of magnetic field sweeps with a systematic variation in field sweep rates [18]. Since such experiments can be very time-consuming, slow relaxation is often ignored or goes unnoticed. We here show that a current-reversal method widely used for sensitive magnetotransport and AHE measurements [21,22] allows us to straightforwardly screen for the presence of slow magnetization relaxation processes. The screening benefits from the slow timescale of the current-reversal measurement as compared to conventional lock-in measurements and provides quantitative access to the normalized relaxation parameter $\mathrm{d}M_{\mathrm{norm}}/\mathrm{d}t$ [with the normalized magnetization $M_{\mathrm{norm}} = M(H)/M_s$ and the saturation magnetization M_s]. In turn, if unaccounted for, then relaxation effects can result in measurement artifacts.

This paper is structured in the following way: In Sec. II we introduce the current-reversal method and derive the effects of slow magnetic relaxation on this method. In Sec. III we apply the current-reversal method to a Pt/Co/AlO_x trilayer showing slow magnetic relaxation to corroborate the considerations from Sec. II. We then compare the dc current-reversal method to the ac lock-in method in Sec. IV and finally apply the method to τ-MnAl as a material of current interested in Sec. V.

II. CURRENT-REVERSAL METHOD

Generally, the current-reversal method (in the following also called delta method) is a standard technique to reduce or

even eliminate thermoelectric voltages from electrical transport measurements [22–24]. In this current-bias, four-point measurement method, for each measurement point two data points are recorded: one voltage $V(+I)$ for positive current polarity and one voltage $V(-I)$ for negative current polarity. The delta-minus signal $V_{\Delta-}$ and delta-plus signal $V_{\Delta+}$ are then calculated as:

$$V_{\Delta-} = \frac{V(+I) - V(-I)}{2} \tag{1}$$

and

$$V_{\Delta+} = \frac{V(+I) + V(-I)}{2}, \tag{2}$$

respectively. Consequently, $V_{\Delta-}$ contains all effects odd in current, such as the resistive contribution. For many experiments focused on (magneto-)resistance, this is the only quantity of interest. In turn, $V_{\Delta+}$ contains all effects even in current, in particular the above mentioned thermoelectric effects. While thermoelectric contributions are often neglected in transport measurements, $V_{\Delta+}$ has proven very useful in the study of, e.g., the spin Seebeck effect [25–27] or spin torque effects [28,29]. In the following, we demonstrate that the $V_{\Delta+}$ signal can also be used to screen for slow relaxation processes.

We now focus on the application of the current-reversal method to field-dependent Hall measurements and the consequences of slow magnetic relaxation effects on these measurements. Phenomenologically, the Hall voltage V_{H} in a ferromagnet with Hall bar or Hall cross shape is described by [30–32]:

$$V_{\mathrm{H}} = \frac{I}{d} \times A_{\mathrm{OHE}} \times \mu_0 H_{\mathrm{ext}} + \frac{I}{d} \times A_{\mathrm{AHE}} \times \mu_0 M(H_{\mathrm{ext}}) \tag{3}$$

with the sourced current I, the ordinary and anomalous Hall coefficients A_{OHE} and A_{AHE}, the external magnetic field H_{ext}, and the sample thickness d. In Hall voltage measurements, voltage offsets due to a geometrical misalignment of the voltage probes or similar artifacts are commonplace [33,34]. This offset is often subtracted from the data without further consideration. Moreover, also a classical planar Hall effect (PHE)—a transversal anisotropic magnetoresistance—contribution could be present in the measured transversal "Hall" voltage [35,36]. This classical PHE contribution would depend on the magnetization orientation, but in contrast to the AHE it would be even under the reversal of magnetic field. For simplicity, we assume that the AHE is much larger than the PHE in the following, which is reasonable for a ferromagnet with high PMA, such that the latter can be neglected [29,35].

To formally model the role of slow magnetic relaxation on the current-reversal method, the time-dependent relaxation of the magnetization $M(t)$ must be taken to account. Owing to the relaxation, the magnetization at times t and $t + \Delta t$ can differ, as approximated by a first-order Taylor expansion:

$$M(t + \Delta t) = M(t) + \frac{\mathrm{d}M}{\mathrm{d}t} \times \Delta t + \mathcal{O}(\Delta t^2). \tag{4}$$

Here the derivative $\mathrm{d}M/\mathrm{d}t$, which we will call relaxation parameter in the following, describes the relaxation. Using Eqs. (2) and (3), the voltage in the delta-plus signal becomes

$$V_{\mathrm{H},\Delta+}\left(t + \frac{\Delta t}{2}\right) = \frac{V_{\mathrm{H}}(t, +I) + V_{\mathrm{H}}(t + \Delta t, -I)}{2} \tag{5}$$

Note that we use $t + \Delta t/2$ as time point for the delta-plus voltage $V_{\mathrm{H},\Delta+}$ since the value is calculated from voltages measured at the time points t and $t + \Delta t$ with Δt being the time between the two voltage readings. Using Eqs. (3)–(5), we can therefore write:

$$\begin{aligned} V_{\mathrm{H},\Delta+}\left(t + \frac{\Delta t}{2}\right) &= -\frac{I}{2d} A_{\mathrm{AHE}} \mu_0 \left.\frac{\mathrm{d}M}{\mathrm{d}t}\right|_{t+\Delta t/2} \Delta t \\ &= -\frac{1}{2} \left.\frac{\mathrm{d}V_{\mathrm{H}}}{\mathrm{d}t}\right|_{t+\Delta t/2} \Delta t. \end{aligned} \tag{6}$$

We stress that the negative sign in Eq. (6) comes from the fact that the first measurement point (at time t) is taken with a positive current polarity, while the second measurement point (at time $t + \Delta t$) is taken for a negative current polarity. Instead of the voltage, one can also consider the resistance $R_{\mathrm{H},\Delta+} = V_{\mathrm{H},\Delta+}/|I|$ calculated from this voltage, which then is as follows:

$$\begin{aligned} R_{\mathrm{H},\Delta+}\left(t + \frac{\Delta t}{2}\right) &= -\frac{1}{2d} A_{\mathrm{AHE}} \mu_0 \left.\frac{\mathrm{d}M}{\mathrm{d}t}\right|_{t+\Delta t/2} \Delta t \\ &= -\frac{1}{2} \left.\frac{\mathrm{d}R_{\mathrm{H}}}{\mathrm{d}t}\right|_{t+\Delta t/2} \Delta t. \end{aligned} \tag{7}$$

Equations (6) and (7) imply that the delta-plus signal allows us to quantify the relaxation parameter $\mathrm{d}M/\mathrm{d}t$ (or rather the normalized relaxation parameter $\mathrm{d}M_{\mathrm{norm}}/\mathrm{d}t$), i.e., the presence and amplitude of slow relaxation in a magnetic conductor, given that the timescale of the relaxation is sufficiently large compared to the time step Δt and that the signal $\mathrm{d}V_{\mathrm{H}}/\mathrm{d}t \times \Delta t$ is above the noise floor of the voltage measurement. It is important to stress that the time it takes to acquire a single voltage reading can be fast. In the discussion above, we thus have tacitly assumed that the voltage reading is instantaneous, while a finite waiting time Δt separates the two measurement points with opposite current polarity. In current-reversal measurements, typical voltage acquisition times range from 0.2 to 1 s, while the delay Δt is of the order of several seconds (see Secs. III and V). The voltage acquisition thus is fast compared to Δt. If the time required to acquire one voltage reading becomes comparable to Δt, then relaxation also will impact the voltage reading itself, and the simple Eqs. (6)–(14) are no longer applicable. However, qualitatively, the delta-plus signal will still show the characteristic signatures of relaxation.

Another important question is Which quantitative information can be extracted from the delta-plus signal in the Hall resistance. Considering the Hall voltage given by Eq. (3), the anomalous Hall signal is proportional to the magnetization and the OHE proportional to the external magnetic field. Therefore it is possible to determine the OHE contribution by fitting a linear function to the Hall voltages at high magnetic fields (i.e., in magnetic saturation) and to remove the OHE by subtraction. Since the AHE contribution is proportional to the (out-of-plane) magnetization component of the sample, we can therefore calculate a normalized AHE signal, which is equivalent to the normalized magnetization M_{norm} [37]:

$$M_{\mathrm{norm}}(H) = \frac{M(H)}{M_s} = \frac{R_{\mathrm{AHE}}(H)}{R_{\mathrm{AHE,s}}} \tag{8}$$

with the field-dependent magnetization $M(H)$, the saturation magnetization M_s, the field-dependent anomalous Hall resistance $R_{\mathrm{AHE}}(H)$, and the anomalous Hall resistance at saturation $R_{\mathrm{AHE,s}}$. In this way, the transport experiments yield $\mathrm{d}M_{\mathrm{norm}}/\mathrm{d}t$ as a quantitative measure of relaxation. Using Eq. (8) and the expression for $R_{\mathrm{H},\Delta+}$ [see Eq. (7)]:

$$R_{\mathrm{H},\Delta+} = -\frac{1}{2}\frac{\mathrm{d}R_{\mathrm{H}}}{\mathrm{d}t}\Delta t, \tag{9}$$

we obtain:

$$\frac{\mathrm{d}M_{\mathrm{norm}}}{\mathrm{d}t} = \frac{\mathrm{d}R_{\mathrm{AHE}}}{\mathrm{d}t}\frac{1}{R_{\mathrm{AHE,s}}} = -2\frac{R_{\mathrm{H},\Delta+}}{R_{\mathrm{AHE,s}}\Delta t}. \tag{10}$$

Note that we hereby have assumed that $\mathrm{d}R_{\mathrm{AHE}}/\mathrm{d}t = \mathrm{d}R_{\mathrm{H}}/\mathrm{d}t$. This is reasonable, since the OHE is time independent (instantaneous on the timescales considered here) and therefore the AHE is the only time-dependent contribution in the Hall resistance. This means we can directly calculate the normalized relaxation parameter $\mathrm{d}M_{\mathrm{norm}}/\mathrm{d}t$ (at the beginning of the relaxation) from the delta-plus signal of the Hall resistance. With knowledge of the saturation magnetization it is further possible to estimate the relaxation parameter $\mathrm{d}M/\mathrm{d}t$. Moreover, using the normalized magnetization from Eq. (8) to calculate a normalized magnetic susceptibility $(\mathrm{d}M_{\mathrm{norm}})/(\mathrm{d}\mu_0 H)$, we estimate the change of the measured coercive field if the magentic field sweep rate is changed:

$$\frac{\mathrm{d}\mu_0 H_{\mathrm{c}}}{\mathrm{d}t} = \left(\frac{\mathrm{d}M_{\mathrm{norm}}}{\mathrm{d}t}\right)\Big/\left(\frac{\mathrm{d}M_{\mathrm{norm}}}{\mathrm{d}\mu_0 H}\right) = \frac{\mathrm{d}M_{\mathrm{norm}}}{\mathrm{d}t} \times \frac{\mathrm{d}\mu_0 H}{\mathrm{d}M_{\mathrm{norm}}}. \tag{11}$$

By analogy to the delta-plus signal, the voltage for the delta-minus signal is as follows:

$$V_{\mathrm{H},\Delta-}(t+\Delta t/2) = \frac{I}{d}\left(A_{\mathrm{OHE}}\mu_0 H_{\mathrm{ext}} + A_{\mathrm{AHE}}\mu_0 M(t) + \frac{1}{2}A_{\mathrm{AHE}}\mu_0\left.\frac{\mathrm{d}M}{\mathrm{d}t}\right|_{t+\Delta t/2}\Delta t\right). \tag{12}$$

Thus,

$$V_{\mathrm{H},\Delta-}(t+\Delta t/2) = V_{\mathrm{H}}(t) + \frac{1}{2}\left.\frac{\mathrm{d}V_{\mathrm{H}}}{\mathrm{d}t}\right|_{t+\Delta t/2}\Delta t \tag{13}$$

and $R_{\mathrm{H},\Delta-} = \frac{V_{\mathrm{H},\Delta-}}{|I|}$:

$$R_{\mathrm{H},\Delta-}(t+\Delta t/2) = R_{\mathrm{H}}(t) + \frac{1}{2}\left.\frac{\mathrm{d}R_{\mathrm{H}}}{\mathrm{d}t}\right|_{t+\Delta t/2}\Delta t. \tag{14}$$

Slow relaxation (finite $\mathrm{d}M/\mathrm{d}t$) thus also results in a finite contribution to the delta-minus signal of the Hall resistance. However this contribution is much smaller than the (time-independent) part of the Hall effect in most materials and thus difficult to resolve.

Finally, substantial relaxation effects typically are observed when the magnetic susceptibility $\mathrm{d}M/\mathrm{d}H$ is large. In a more elaborate model, also the relaxation time constant can depend on the magnetic field strength [5]. We thus expect marked relaxation-related contributions to the delta-plus signal of the Hall resistance $R_{\mathrm{H},\Delta+}$ in the field range for magnetic hysteresis, in which the magnetization (and therefore AHE) is switching.

III. MAGNETIC RELAXATION IN A Pt/Co/AlO$_x$ THIN-FILM HETEROSTRUCTURE

In order to experimentally corroborate the consideration in Sec. II, we study the magnetotransport response of a trilayer consisting of 5 nm platinum, 1.1 nm cobalt, and 1.6 nm aluminum oxide sputter-deposited onto a silicon substrate with thermal silicon oxide. We refer to this trilayer as Pt/Co/AlO$_x$. The heterostructure is patterned into Hall crosses, as described in more detail by Nabben *et al.* [38]. We measure the Hall effect using a room-temperature electromagnet setup, with the magnetic field applied along the film normal. The current is hereby applied using a Keithley 2450 sourcemeter and the transversal (Hall) voltage is recorded by a Keithley 2182A nanovoltmeter.

The sample shows perpendicular magnetic anisotropy, a high remanence, and a deviation from a square hysteresis loop at higher magnetic fields, as evident in the Hall curve in Fig. 1(a). The delta-minus signal of the Hall resistance $R_{\mathrm{H},\Delta-} = V_{\mathrm{H},\Delta-}/|I|$ is dominated by the anomalous Hall contribution [30], the ordinary Hall contribution is negligible in comparison [see left axis of Fig. 1(a)]. Similar hysteresis curves were observed in other Co/Pt layers, as, for example, described by Shen *et al.* for Co/Pt multilayers consisting of 30 stacks. These authors also attribute the shape of the hysteresis loop to nonuniform domain wall expansion [39]. We expect similar effects in our Pt/Co/AlO$_x$ film. We intentionally did not remove the offset in the Hall measurements discussed above in Sec. II. The right axis of Fig. 1(a) shows the normalized magnetization of the sample calculated with Eq. (8). As described in detail in Sec. S1 of the Supplemental Material [40], the magnetic hysteresis inferred from the Hall transport data is corroborated by SQUID magnetometry experiments. We now consider the delta-plus signal of the Hall resistance $R_{\mathrm{H},\Delta+} = V_{\mathrm{H},\Delta+}/|I|$ shown in Fig. 1(b) (left axis), obtained from the same set of data as $R_{\mathrm{H},\Delta-}$, simply by adding instead of subtracting subsequent voltage measurements. As expected from the discussion in Sec. II we indeed observe a finite signal. As we perform magnetic field sweeps, i.e., we record the Hall voltage for increasing (up-sweep) and decreasing (down-sweep) magnetic field amplitude, we can further plot $(\mathrm{d}R_{\mathrm{H},\Delta-})/(\mathrm{d}\mu_0 H)$ as a measure for the magnetic susceptibility $(\mathrm{d}M)/(\mathrm{d}H)$ in the left axis of Fig. 1(c) and obtain a sharp peak followed by a broad shoulder in the magnetic field ranges in which the magnetization reorients, which is qualitatively similar to the delta-plus signal $R_{\mathrm{H},\Delta+}$ in Fig. 1(b). The magnetic field sweep direction is hereby encoded in the sign of $R_{\mathrm{H},\Delta+}$, while $(\mathrm{d}R_{\mathrm{H},\Delta-})/(\mathrm{d}\mu_0 H)$ is not affected by the sweep direction, since the time axis is irrelevant here. Moreover, we have carefully checked that the delta-plus signal shows an ohmic behavior, i.e., delta-plus signal of the Hall resistance $R_{\mathrm{H},\Delta+}$ is constant for different magnitudes of the sourced current I. This together with the signal's shape rules out the possibility of a thermal origin. Nevertheless, similar effects could be misinterpreted as thermovoltages if the delta method is used to intentionally measure thermovoltages. In Figs. 1(b) and 1(c), the position and magnitude of the peaks are not symmetrical. This is due to the fact that in our setup, we apply a series of current levels to the coils of the electromagnet to generate different magnetic field values. Owing

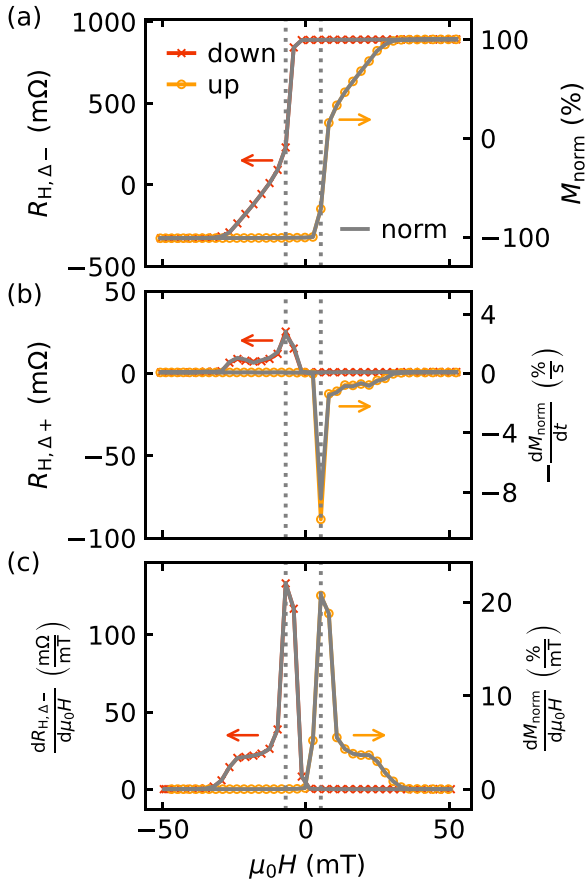

FIG. 1. Hall resistance of Pt/Co/AlO_x, recorded using the delta method. (a) Left axis: delta-minus signal of the Hall resistance (symbols); right axis: normalized magnetization calculated from the Hall resistance using Eq. (8) (gray full line). (b) Left axis: delta-plus signal of the Hall resistance (symbols); right axis: negative of (normalized) relaxation parameter dM_{norm}/dt calculated from the delta-plus signal of the Hall resistance, using Eq. (10) (gray full line). (c) Left axis: derivative of the delta-minus signal of the Hall resistance with respect to the external field $\mu_0 H$ (symbols); right axis: normalized susceptibility [derivative $(dM_{norm})/(d\mu_0 H)$ calculated from the normalized magnetization] (gray full line). The data were recorded with a time step $\Delta t = 3\,s$ and $I = 1\,mA$ at room temperature. The field sweep directions are indicated by arrows and different symbol shapes and colors.

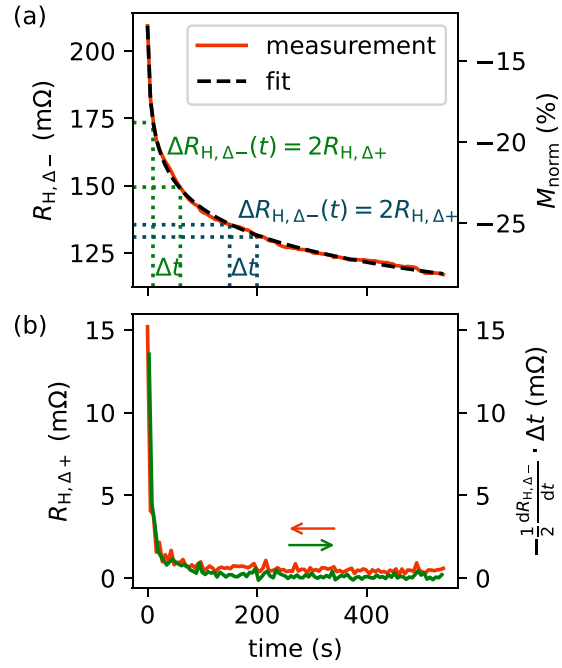

FIG. 2. Time-dependent evolution of the Hall resistance in the Pt/Co/AlO_x film at $\mu_0 H = -7\,mT$. (a) Left axis: measured time trace of the delta-minus signal of the Hall resistance, with schematic depiction of the link between $R_{H,\Delta-}$ and $R_{H,\Delta+}$ in the delta method with exaggerated time steps Δt; right axis: time trace of normalized magnetization calculated from $R_{H,\Delta-}$ using Eq. (8). The relaxation is fitted with a logarithmic function [cf. Eq. (19)] as depicted as the black dashed line. (b) Left axis: measured time trace of the delta-plus signal of the Hall resistance (red) and right axis: derivative $-\frac{1}{2}dR_{H,\Delta-}/dt$ (green) calculated via Eq. (7).

to the finite remanence of the iron yoke of the magnet, this results in slightly different applied magnetic fields for positive and negative currents in the coils. Since the peaks are very narrow, small deviations in the magnetic field can have a big influence on the measured value. Additionally, the reason for the qualitative difference of the two-step variation with H in Figs. 1(b) and 1(c) could be a field-dependent time constant of the relaxation.

The negative of the normalized relaxation parameter dM_{norm}/dt [see Eq. (10)] is shown in the right axis of Fig. 1(b). It goes up to approximately 8%/s at the sharp peak and is in the order of 0.8 %/s in the region of the shoulders. In the right axis of Fig. 1(c) we plot the normalized susceptibility $(dM_{norm})/(d\mu_0 H)$. With the approximation from Eq. (11), the normalized relaxation parameter dM_{norm}/dt and the normalized susceptibility $(dM_{norm})/(d\mu_0 H)$ [see right axis of Fig. 1(c)] we can therefore estimate the sensitivity of the measured coercive field with regard to small changes of the field sweep rate or measurement delays as up to approximately 0.4 mT/s, for a coercive field of approximately 7 mT. Here the derivative dH_c/dt is in the same order of magnitude as the coercive field. Therefore changes of the field sweep rate will have a noticeable impact on the measurement of the coercive field. To confirm that the delta-plus signal of the Hall resistance originates from slow magnetic relaxation, we measure a time trace of both the delta-plus and delta-minus signal of the Hall resistance. In these measurements, we first saturate the magnetization of the thin film by applying a magnetic field of 50 mT. Then we sweep the magnetic field to a given magnetic field value near to the coercive field (i.e., −7 mT in Fig. 2). Now the magnetic field is kept constant and the voltage $V(t)$ is recorded over time, using the delta method. The investigated Pt/Co/AlO_x films indeed exhibit a slow magnetic relaxation as shown by the time trace of the delta-minus signal of the Hall resistance $R_{H,\Delta-}$ in Fig. 2(a). In the time trace of the delta-plus signal of the Hall resistance $R_{H,\Delta+}$, depicted in Fig. 2(b) (red curve), we observe a finite signal which decays over time. This decay is equivalent to the quantity $-\frac{1}{2}dR_H/dt\,\Delta t$ calculated in Eq. (7) and can be seen by comparing the red and green curve in Fig. 2(b). Note that in Eq. (7) we have the derivative dR_H/dt, while in Fig. 2(b) the derivative $dR_{H,\Delta-}/dt$ is plotted.

TABLE I. Fit parameters of the logarithmic decay, Eq. (19), used to fit the time evolution of the normalized magnetization in the Pt/Co/AlO_x sample in Fig. 2(a).

Parameter	Value
M_{norm}	−12.86(11)%
S_{norm}	2.402(14)%
t_0	0.93(6) s

Strictly speaking, these two terms are not equivalent. We can write the time derivative of Eq. (14) as:

$$\frac{\mathrm{d}R_{\mathrm{H},\Delta-}}{\mathrm{d}t} = \frac{\mathrm{d}R_{\mathrm{H}}}{\mathrm{d}t} + \frac{1}{2}\frac{\mathrm{d}^2R_{\mathrm{H},\Delta-}}{\mathrm{d}t^2}\Delta t. \tag{15}$$

If we transpose Eq. (15) to $\frac{\mathrm{d}R_{\mathrm{H}}}{\mathrm{d}t}$ and use this term in Eq. (7), then we obtain:

$$R_{\mathrm{H},\Delta+}(t+\Delta t/2) = -\frac{1}{2}\frac{\mathrm{d}R_{\mathrm{H},\Delta-}}{\mathrm{d}t}\bigg|_{t+\Delta t/2}\Delta t + \frac{1}{2}\frac{\mathrm{d}^2R_{\mathrm{H},\Delta-}}{\mathrm{d}t^2}\bigg|_{t+\Delta t/2}(\Delta t)^2. \tag{16}$$

This corresponds to a second-order Taylor expansion in analogy to the first-order Taylor expansion in Eq. (4). Given that $|\frac{1}{2}\mathrm{d}^2R_{\mathrm{H},\Delta-}/\mathrm{d}t^2 \times (\Delta t)^2| \ll |\frac{1}{2}\mathrm{d}R_{\mathrm{H},\Delta-}/\mathrm{d}t \times \Delta t|$, which is the case if the time step Δt is sufficiently smaller than the timescale on which the relaxation happens, we can neglect the second-order term, thus:

$$R_{\mathrm{H},\Delta+}(t+\Delta t/2) = -\frac{1}{2}\frac{\mathrm{d}R_{\mathrm{H},\Delta-}}{\mathrm{d}t}\bigg|_{t+\Delta t/2}\Delta t. \tag{17}$$

As shown by the agreement of the red and green curves in Fig. 2(b), the timescale of the relaxation is slow enough compared to the time step Δt to assume that $\mathrm{d}R_{\mathrm{H}}/\mathrm{d}t = \mathrm{d}R_{\mathrm{H},\Delta-}/\mathrm{d}t$. In summary, the measurements on the Pt/Co/AlO_x trilayer confirm the considerations from Sec. II. Slow magnetic relaxation leads to a measurable delta-plus signal of the Hall resistance, as shown in Fig. 1(b).

Slow magnetic relaxation can be described by different models. In many cases a logarithmic decay of the shape:

$$M(t) = M(t=0) - S\ln(1+t/t_0) \tag{18}$$

with the time-dependent magnetization $M(t)$, the magnetization at the beginning of the decay $M(t=0)$, the magnetic viscosity S, and the fit parameter t_0, describes the magnetic relaxation well [10,12,41]. We modify this equation to use the normalized magnetization M_{norm} as:

$$M_{\mathrm{norm}}(t) = M_{\mathrm{norm}}(t=0) - S_{\mathrm{norm}}\ln(1+t/t_0), \tag{19}$$

which also leads to a normalized magnetic viscosity S_{norm}. We fit this logarithmic decay to the time trace of the normalized magnetization in Fig. 2(a). The fit (black dashed line) matches well with the data. The fit parameters are compiled in Table I. As Eq. (17) predicts that the delta-plus signal of the Hall resistance probes the derivative of the magnetization, and the magnetization decays in a logarithmic fashion with time, the delta-plus signal decays much faster [i.e., with $R_{\mathrm{H},\Delta+} \propto \mathrm{d}M(t)/\mathrm{d}t = -S/(t_0+t)$] than the delta-minus signal of the Hall resistance, which is proportional to the magnetization. Note also that, for comparison, we investigate the slow magnetic relaxation on another piece from the same Pt/Co/AlO_x trilayer using SQUID magnetometry. Time traces and the corresponding logarithmic fits are shown in Sec. S2 of the Supplemental Material [40]. The SQUID magnetomtery and Hall effect data show a similar behavior.

IV. COMPARISON TO THE LOCK-IN METHOD

Another standard method for sensitive (magneto-) resistance measurements and the investigation of higher harmonic signals is homodyne detection using a lock-in amplifier. In the following, we discuss whether lock-in based Hall measurements are equally susceptible to slow relaxation effects. Instead of a dc current, we thus consider that an ac current $I_{\mathrm{lock-in}}$ with a reference frequency f_{ref}, the angular frequency $\omega = 2\pi f_{\mathrm{ref}}$, and an amplitude I_0 is applied [42,43]:

$$I_{\mathrm{lock-in}} = I_0\cos(2\pi f_{\mathrm{ref}}t) = I_0\cos(\omega t). \tag{20}$$

The measured ac voltage V_m can then be demodulated with respect to different frequencies and phase shifts so that the in-phase components V_x and the quadrature components V_y of the first harmonic signal V^{ω} and the second harmonic signal $V^{2\omega}$ can be extracted. From Eqs. (3) and (20), it follows that the slow magnetic relaxation manifests as a decreasing or increasing envelope of the measured ac Hall voltage V_m (depending on sweep direction and Hall sign). Due to the changing envelope, the peak at 1ω in Fourier/frequency space is expected to broaden, when a magnetic relaxation is present.

$$V_m = (A_{\mathrm{OHE}}\mu_0 H_{\mathrm{ext}} + A_{\mathrm{AHE}}\mu_0 M(H_{\mathrm{ext}},t))\frac{I_0}{d}\cos(\omega t) \tag{21}$$

Therefore, after demodulation with $\cos(\omega t)$ for the in-phase first harmonic of the Hall resistance $R^{\omega}_{\mathrm{H},x} = V^{\omega}_{\mathrm{H},x}/I_0$ in both cases the demodulated signal (e.g., first harmonic of the Hall resistance) is dominated by the time-independent part of the Hall signal. For the first harmonic quadrature component $R^{\omega}_{\mathrm{H},y} = V^{\omega}_{\mathrm{H},y}/I_0$ and the in-phase second harmonic component $R^{2\omega}_{\mathrm{H},x} = V^{2\omega}_{\mathrm{H},x}/I_0$ the measured voltage signal is demodulated with $\sin(\omega t)$ and $\cos(2\omega t)$, respectively. Therefore in the absence of slow magnetic relaxation, the first harmonic quadrature component $R^{\omega}_{\mathrm{H},y}$ and second harmonic in-phase component $R^{2\omega}_{\mathrm{H},x}$ vanish. The residual signals in these components that occur when the magnetic system relaxes is similar to the delta-plus signal of the Hall resistance in the dc current-reversal method. In addition, irrespective of whether magnetization relaxation is present, the second harmonic signal can also have contributions from thermoelectric effects, in analogy to the discussion for the dc method. To verify these considerations, we performed lock-in measurements on the Pt/Co/AlO_x Hall crosses. In Figs. 3(a), 3(c), and 3(e) we show measurements at a slow reference frequency $f_{\mathrm{ref}} =$ 1 Hz. However, in many lock-in measurements higher reference frequencies are used to shift the detection window away from $1/f$ noise, which is large at low f [44,45]. We therefore also show measurements at a more commonly used reference frequency of 89 Hz in Figs. 3(b), 3(d), 3(f), and 3(g), using a phase correction of $\theta_{\mathrm{cor}} = -0.019$ rad, to compensate for reactive effects in the circuit. The time constant for the lock-in

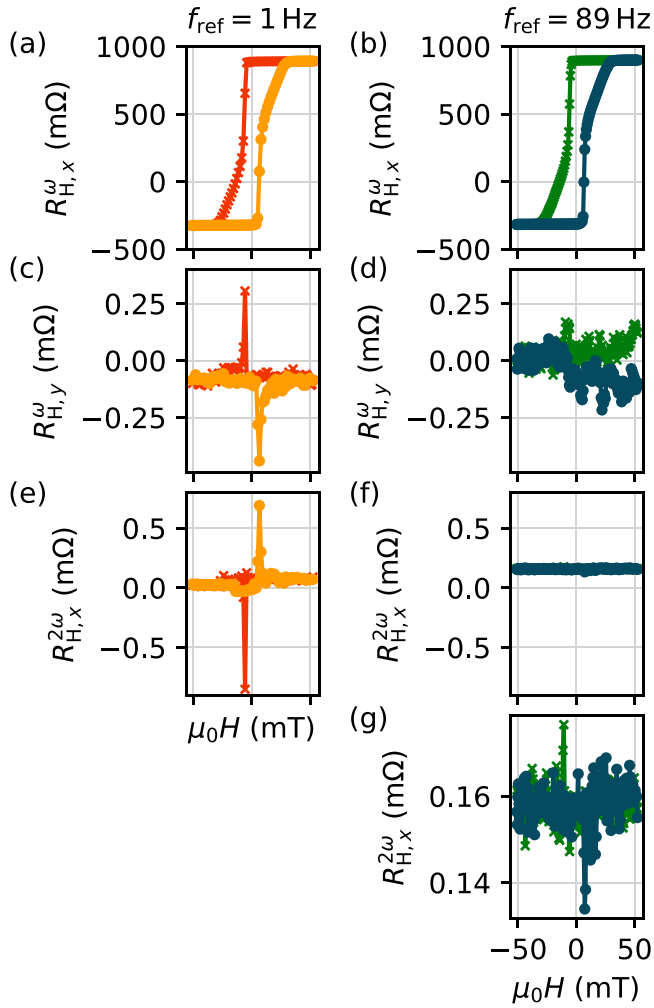

FIG. 3. Hall resistance of Pt/Co/AlO_x recorded using the lock-in scheme. [(a) and (b)] In-phase component of the first harmonic of the Hall resistance. [(c) and (d)] Quadrature component of the first harmonic of the Hall resistance. [(e) and (f)] In-phase component of the second harmonic of the Hall resistance. (g) Zoomed plot of the in-phase component of the second harmonic of the Hall resistance, recorded with $f_{ref} = 89$ Hz. Panels (a), (c), and (e) show the measurements with a reference frequency of 1 Hz. Panels (b), (d), (f), and (g) show the measurements with a reference frequency of 89 Hz. The data were recorded at room temperature.

measurements at $f_{ref} = 1$ Hz was chosen as 3 s, while the time constant for the measurement at $f_{ref} = 89$ Hz was chosen as 1 s. For both reference frequencies, a clear Hall signal is present in the in-phase component of the first harmonic of the Hall resistance [see Figs. 3(a) and 3(b)]. For $f_{ref} = 89$ Hz, we see no signature of the slow relaxation in the quadrature component of the first harmonic of the Hall resistance [Fig. 3(d)]. Moreover, also the in-phase component of the second harmonic of Hall the resistance [Figs. 3(f) and 3(g)] apparently is not affected by relaxation but rather dominated by leakage of the first harmonic component into the second harmonic component by insufficient filtering or harmonic distortion. For $f_{ref} = 1$ Hz, small but clear signatures of the slow relaxation in both the quadrature component of the first harmonic of the Hall resistance [Fig. 3(c)] and the in-phase component of the second harmonic of the Hall resistance [Fig. 3(e)] appear, as expected. Hence, the lock-in method is rather robust against measurement artifacts stemming from slow magnetic relaxation effects, at least for reference frequencies $f_{ref} \gtrapprox 100$ Hz, which are much faster than the typical slow (seconds and longer) relaxation rates [46,47]. The influence of the integration time τ and reference frequency f_{ref} on the different components of the lock-in outputs are discussed using a simple numerical model in Sec. S3 of the Supplemental Material [40].

V. MAGNETIC RELAXATION IN MnAl THIN FILMS

We now use the current-reversal method to gauge the presence of magnetic relaxation in a material of current interest, τ-MnAl. This ferromagnetic compound features a high uniaxial magnetocrystallline anisotropy [48], making it a potential candidate for a PMA material in spintronic applications such as spin transfer torque MRAM [49–52]. Furthermore, it is actively investigated for its potential as a rare-earth free permanent magnet [52–54]. Slow magnetic relaxation processes have recently been observed in ferromagnetic τ-Mn-Al-C alloys [12] as well as bulk Mn-Ga and Mn-Al alloys [55]. We here focus on a 78-nm-thick MnAl film sputter-deposited onto a 19-nm-thick Cr buffer layer on a MgO(001) substrate. Details of the growth parameters of the film are described by Scheffler *et al.* [56]. The film is patterned into a Hall bar by optical lithography and wet etching. The Hall response is measured in a superconducting magnet cryostat with variable temperature insert, since the coercive field of MnAl is much higher than the coercive field of the Pt/Co/AlO_x film. Again, the current is applied using a Keithley 2450 sourcemeter and the transversal voltage measured with a Keithley 2182A nanovoltmeter. All data discussed in the following were taken with the sample at room temperature. In Fig. 4(a) we show the Hall resistance (recorded using the delta method) in dependence of the external magnetic field. In Fig. 4(b) (left axis) the OHE contribution is removed from the Hall measurements, as described in Sec. II, such that only the delta-minus signal of the anomalous Hall resistance remains. On the right axis the normalized magnetization is depicted, which is calculated using Eq. (8). Again, the accordance of the hysteresis curve measured by SQUID magnetometry with the hysteresis curve measured with the Hall effect is demonstrated in Sec. S1 of the Supplemental Material [40]. The delta-plus signal of the Hall resistance is shown in the left axis of Fig. 4(c). This signal shows clear peaks when the magnetization reorients, indicating the presence of slow relaxation of the magnetization. As can be seen on the left axis of Fig. 4(d) the maxima of the delta-plus signal again coincide with the maximum change of Hall resistance and therefore maximum change of magnetization (i.e., maximal susceptibility) in the sample. In the right axis of Fig. 4 the negative of the normalized relaxation parameter $\mathrm{d}M_{\mathrm{norm}}/\mathrm{d}t$ is depicted, obtained using Eq. (10). Here the maximum of the normalized relaxation parameter is approximately 0.4%/s. This normalized relaxation parameter is an order of magnitude smaller compared to the 8%/s observed in the Pt/Co/AlO_x trilayer. We therefore expect, that the timescale of relaxation in the MnAl sample is higher (i.e., slower relaxation) compared to the Pt/Co/AlO_x sample.

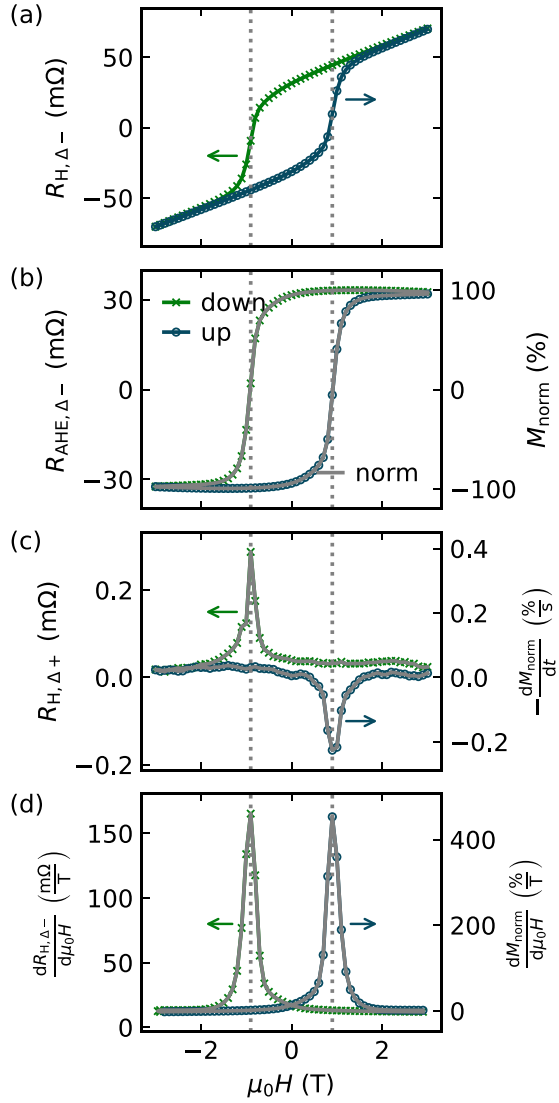

FIG. 4. Magnetic relaxation in a MnAl thin film detected via the delta method. (a) Delta-minus signal of the Hall resistance. (b) Left axis: delta-minus signal of the anomalous Hall resistance obtained by subtracting the OHE from the data in (a) (symbols); right axis: normalized magnetization calculated from the anomalous Hall resistance, using Eq. (8) (gray full line). (c) Left axis: delta-plus signal of the Hall resistance (symbols); right axis: negative of the (normalized) relaxation parameter $\mathrm{d}M_{\mathrm{norm}}/\mathrm{d}t$ calculated from the delta-plus signal of the Hall resistance via Eq. (10) (gray full line). (d) Left axis: Derivative of the delta-minus signal of the Hall resistance with respect to the external field $\mu_0 H$. (Symbols) Right axis: normalized susceptibility (derivative $\mathrm{d}M_{\mathrm{norm}}/\mathrm{d}\mu_0 H$ calculated from the normalized magnetization) (gray full line). The data were recorded with sample held at a temperature of $T = 300\,\mathrm{K}$, with a time step $\Delta t = 4.5\,\mathrm{s}$ and a current of $I = 5\,\mathrm{mA}$. The field sweep directions are indicated by arrows and different symbol colors.

Using the approximation from Eq. (11), the normalized relaxation parameter $\mathrm{d}M_{\mathrm{norm}}/\mathrm{d}t$ [see right axis Fig. 4(c)], and the normalized susceptibility $\mathrm{d}M_{\mathrm{norm}}/\mathrm{d}\mu_0 H$ [see right axis of Fig. 4(d)] we can estimate the sensitivity of the measured coercive field with regard to small changes of the field sweep rate or measurement delays as approximately 0.0009 T/s, which

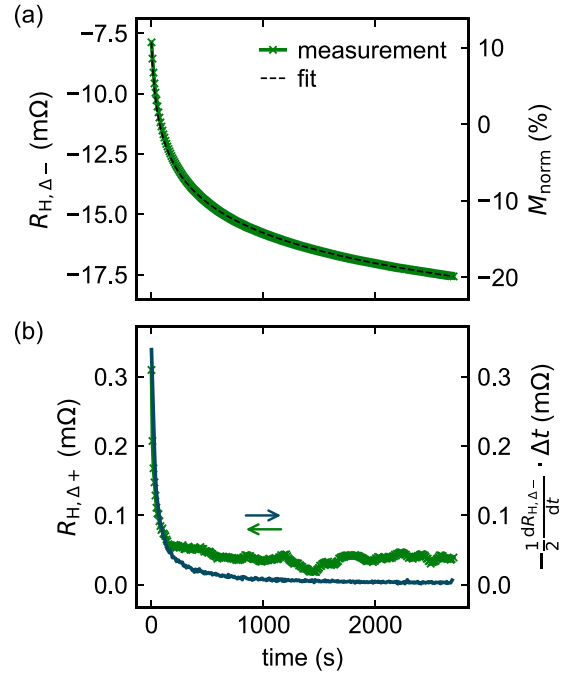

FIG. 5. Time-dependent evolution of the Hall resistance in a MnAl film at $\mu_0 H = -0.9\,\mathrm{T}$. (a) Left axis: measured time trace of the delta-minus signal of the Hall resistance $R_{\mathrm{H},\Delta-}$; right axis: time trace of the normalized magnetization calculated from $R_{\mathrm{H},\Delta-}$ using Eq. (8). The relaxation is fitted with a logarithmic function [cf. Eq. (19)] depicted as a black dashed line. (b) Left axis: measured time trace of the delta-plus signal of the Hall resistance (green symbols); right axis: derivative $-\frac{1}{2}\mathrm{d}R_{\mathrm{H},\Delta-}/\mathrm{d}t$ (blue) calculated via Eq. (7).

is negligible small compared to the coercive field $H_c \approx 0.9\,\mathrm{T}$. Therefore we expect no noticeable influence of (reasonable) changes of the field sweep rate on the measurement of the coercive field. To confirm this assumption, we measured a time trace of the transversal voltage. Like in Sec. III for this measurement, first the magnetization of the sample is saturated at a high (positive) magnetic field after which the external field is ramped to a negative field value (i.e., $-0.9\,\mathrm{T}$) and then kept constant. Once the field is stable, the voltage is recorded over time using the delta method. In Fig. 5(a) we show the delta-minus signal of the Hall resistance over time for this measurement. The normalized magnetization values corresponding to this Hall resistances are depicted in the right axis. Figure 5(b) shows the delta-plus signal of the Hall resistance on the left axis (green curve) and the correspondence of this values to the term $-\frac{1}{2}\mathrm{d}R_{\mathrm{H},\Delta-}/\mathrm{d}t \times \Delta t$ [see Eq. (7)] on the right axis (blue curve). Note that the curves only match until a time of approximately 150 s. After this time, the measured curve is dominated by noise, since the calculated voltage is beneath the noise floor of the experimental setup. We also fit the logarithmic decay [cf. Eq. (19)] to the time trace of the normalized magnetization in Fig. 5(a) (black dashed line). The fit parameters are compiled in Table II. We show additional current-reversal measurements at lower sample temperatures in Sec. S4 of Supplemental Material, and field-dependent time traces in Sec. S5 of Supplemental Material [40]. These measurements suggest, that the relaxation in MnAl can be

TABLE II. Fit parameters of the logarithmic decay, Eq. (19), used to fit the time evolution of the normalized magnetization in the MnAl film in Fig. 5(a).

Parameter	Value
M_{norm}	10.69(9)%
S_{norm}	5.766(10)%
t_0	13.5(29) s

well described by the Preisach model [41], similarly to the observations of Volegov *et al.* in bulk MnAl [55]. However, as evident from the measurement curve, the relaxation in the MnAl thin film happens on a much longer timescale (cf. time axis in Fig. 5) as compared to the relaxation in the $Pt/Co/AlO_x$ trilayer (see time axis in Fig. 2). We observe the different timescales also in the fits of the logarithmic decay. The fit parameter $t_0 = 0.93$ s for $Pt/Co/AlO_x$ is much shorter than the value of $t_0 = 13.5$ s for MnAl. This corroborates the notion that the current-reversal method allows us to detect the (normalized) relaxation parameter and subtle changes in slow magnetic relaxation. In particular, in field sweep rate-dependent measurements on MnAl, such subtle changes could easily be overlooked, highlighting a big advantage of the current-reversal method.

VI. SUMMARY AND OUTLOOK

In conclusion, we presented a scheme for the detection of slow magnetic relaxation effects based on the measurement of the AHE response via a standard dc current-reversal method. This method can easily be applied to standard Hall measurements and is very sensitive to even subtle slow relaxation processes. As such, it is an ideal technique for fast screening, providing first information about the timescale and amplitude of slow relaxation processes, quantify $\mathrm{d}M_{\mathrm{norm}}/\mathrm{d}t$, and identify field ranges for further investigation of the relaxation processes in magnetic films showing an AHE. Therefore, the method is also well suited to screen sample series and investigate the influence of parameters such as induced substrate strain or chemical composition on the magnetic aftereffect. Our analysis reveals that the method is ideally suited to study relaxation processes on the timescale of a few seconds up to several hundred seconds. For such relaxation parameters, conventional lock-in based magnetotransport measurements are much less sensitive to relaxation effects. In other words, the dc delta method has the advantage, that it works at very low frequencies, for which lock-in schemes are overwhelmed by $1/f$ noise.

ACKNOWLEDGMENTS

This work was funded by the Deutsche Forschungsgemeinschaft (DFG, German Research Foundation) projects ID 445976410 and ID 490730630 and via the SFB 1432 Project-ID 425217212. This work was supported by the French national research agency (ANR) Project ID ANR-20-CE92-0049-01. D.K. acknowledges the Czech Academy of Sciences (Project No. LQ100102201). H.R. was supported by the Grant Agency of the Czech Republic Grant No. 22-17899K and via the Dioscuri Program by Max Planck Society and the Ministry of Education, Youth and Sports of the Czech Republic.

[1] F. Preisach, Über die magnetische Nachwirkung, Z. Phys. **94**, 277 (1935).
[2] Louis Néel, Le traînage magnétique, J. Phys. Radium **12**, 339 (1951).
[3] E. P. Wohlfarth, The coefficient of magnetic viscosity, J. Phys. F: Met. Phys. **14**, L155 (1984).
[4] G. Bayreuther, P. Bruno, G. Lugert, and C. Turtur, Magnetic aftereffect in ultrathin ferromagnetic films, Phys. Rev. B **40**, 7399(R) (1989).
[5] M. Labrune, S. Andrieu, F. Rio, and P. Bernstein, Time dependence of the magnetization process of RE-TM alloys, J. Magn. Magn. Mater. **80**, 211 (1989).
[6] J. Pommier, P. Meyer, G. Pénissard, J. Ferré, P. Bruno, and D. Renard, Magnetization reversal in ultrathin ferromagnetic films with perpendicular anisotropy: Domain observations, Phys. Rev. Lett. **65**, 2054 (1990).
[7] J. Thiele, J. Ferré, P. Meyer, C. Guillot, R. Belkhou, and N. Barrett, Kerr study of Pt/Co/Pt(111) sandwiches, J. Magn. Magn. Mater. **148**, 17 (1995).
[8] R. A. Fry, L. H. Bennett, and E. Della Torre, Magnetic aftereffect in a bimodal Co/Pt magneto-optical medium, J. Appl. Phys. **85**, 5983 (1999).
[9] R. A. Fry, A. Reimers, L. H. Bennett, and E. Della Torre, Preisach modeling of aftereffect in a magneto-optical medium with perpendicular magnetization, Phys. B: Condens. Matter **275**, 50 (2000).
[10] H. Xi, K.-Z. Gao, J. Ouyang, Y. Shi, and Y. Yang, Slow magnetization relaxation and reversal in magnetic thin films, J. Phys.: Condens. Matter **20**, 295220 (2008).
[11] K. X. Xie, W. W. Lin, H. C. Sun, Y. Nie, and H. Sang, Time dependence of magnetization reversal influenced by current in perpendicularly magnetized Co/Pt thin film, J. Appl. Phys. **104**, 083907 (2008).
[12] A. Pasko, A. Pecheux, M. Tyrman, L. Perrière, I. Guillot, V. Etgens, M. LoBue, and F. Mazaleyrat, Temperature dependence of coercivity and magnetic relaxation in a Mn–Al–C permanent magnet, IEEE Trans. Magn. **57**, 1 (2021).
[13] J. Ferré, Dynamics of magnetization reversal: From continuous to patterned ferromagnetic films, in *Spin Dynamics in Confined Magnetic Structures I*, edited by B. Hillebrands and K. Ounadjela (Springer, Berlin, 2002), pp. 127–168.
[14] J. Xu, J. Xia, X. Zhang, C. Zhou, D. Shi, H. Chen, T. Wu, Q. Li, H. Ding, Y. Zhou, and Y. Wu, Exchange-torque-triggered fast switching of antiferromagnetic domains, Phys. Rev. Lett. **128**, 137201 (2022).
[15] Z. Kašpar, M. Surýnek, J. Zubáč, F. Krizek, V. Novák, R. P. Campion, M. S. Wörnle, P. Gambardella, X. Marti, P. Němec, K. W. Edmonds, S. Reimers, O. J. Amin, F. Maccherozzi,

S. S. Dhesi, P. Wadley, J. Wunderlich, K. Olejník, and T. Jungwirth, Quenching of an antiferromagnet into high resistivity states using electrical or ultrashort optical pulses, Nat. Electron. **4**, 30 (2021).

[16] I. S. Weir, J. N. Chapman, D. M. Titterington, and J. Rose, Observation and modelling of magnetization reversal in multilayers supporting perpendicular magnetization, J. Phys. D: Appl. Phys. **32**, 395 (1999).

[17] R. C. Bhatt, L.-X. Ye, L.-R. Lin, N. T. Hai, J.-C. Wu, and T.-H. Wu, Study of slow magnetization relaxation in Hf/GdFeCo/SiN Hall bar by anomalous Hall resistance measurements, J. Magn. Magn. Mater. **564**, 170106 (2022).

[18] D. Kan, T. Moriyama, and Y. Shimakawa, Field-sweep-rate and time dependence of transverse resistivity anomalies in ultrathin $SrRuO_3$ films, Phys. Rev. B **101**, 014448 (2020).

[19] P. J. Flanders and M. Sharrock, An analysis of time-dependent magnetization and coercivity and of their relationship to print-through in recording tapes, J. Appl. Phys. **62**, 2918 (1987).

[20] M. A. Wongsam, J. D. Hannay, G. W. Roberts, and R. W. Chantrell, Recent studies in thermal activation and spin waves, J. Magn. Magn. Mater. **200**, 649 (1999).

[21] M. Asa, C. Autieri, R. Pazzocco, C. Rinaldi, W. Brzezicki, A. Stroppa, M. Cuoco, G. Varvaro, S. Picozzi, and M. Cantoni, Anomalous Hall effect in antiferromagnetic/nonmagnetic interfaces, Phys. Rev. Res. **2**, 043394 (2020).

[22] D. Rüffer, Non-local Phenomena in Metallic Nanostructures, Diploma thesis, Walther-Meißner-Institut, Technische Universität München, 2009.

[23] M. N. Pitsakis and X. Wang, Automated superconductor measurements system, Rev. Sci. Instrum. **60**, 135 (1989).

[24] S. T. B. Goennenwein, R. Schlitz, M. Pernpeintner, K. Ganzhorn, M. Althammer, R. Gross, and H. Huebl, Non-local magnetoresistance in YIG/Pt nanostructures, Appl. Phys. Lett. **107**, 172405 (2015).

[25] M. Schreier, N. Roschewsky, E. Dobler, S. Meyer, H. Huebl, R. Gross, and S. T. B. Goennenwein, Current heating induced spin Seebeck effect, Appl. Phys. Lett. **103**, 242404 (2013).

[26] J. Gückelhorn, T. Wimmer, S. Geprägs, H. Huebl, R. Gross, and M. Althammer, Quantitative comparison of magnon transport experiments in three-terminal YIG/Pt nanostructures acquired via dc and ac detection techniques, Appl. Phys. Lett. **117**, 182401 (2020).

[27] J. Cramer, L. Baldrati, A. Ross, M. Vafaee, R. Lebrun, and M. Kläui, Impact of electromagnetic fields and heat on spin transport signals in $Y_3Fe_5O_{12}$, Phys. Rev. B **100**, 094439 (2019).

[28] A. Manchon, J. Železný, I. M. Miron, T. Jungwirth, J. Sinova, A. Thiaville, K. Garello, and P. Gambardella, Current-induced spin-orbit torques in ferromagnetic and antiferromagnetic systems, Rev. Mod. Phys. **91**, 035004 (2019).

[29] K. Garello, I. M. Miron, C. O. Avci, F. Freimuth, Y. Mokrousov, S. Blügel, S. Auffret, O. Boulle, G. Gaudin, and P. Gambardella, Symmetry and magnitude of spin–orbit torques in ferromagnetic heterostructures, Nat. Nanotechnol. **8**, 587 (2013).

[30] N. Nagaosa, J. Sinova, S. Onoda, A. H. MacDonald, and N. P. Ong, Anomalous Hall effect, Rev. Mod. Phys. **82**, 1539 (2010).

[31] E. M. Pugh and T. W. Lippert, Hall e.m.f. and intensity of magnetization, Phys. Rev. **42**, 709 (1932).

[32] E. M. Pugh and N. Rostocker, Hall effect in ferromagnetic materials, Rev. Mod. Phys. **25**, 151 (1953).

[33] A. Badura, D. Kriegner, E. Schmoranzerová, K. Výborný, M. Leiviskä, R. L. Seeger, V. Baltz, D. Scheffler, S. Beckert, I. Kounta, L. Michez, L. Šmejkal, J. Sinova, S. T. B. Goennenwein, J. Železný, and H. Reichlová, Even-in-magnetic-field part of transverse resistivity as a probe of magnetic order, arXiv:2311.14498 [cond-mat.mes-hall].

[34] J. P. DeGrave, D. Liang, and S. Jin, A general method to measure the Hall effect in nanowires: Examples of FeS_2 and MnSi, Nano Lett. **13**, 2704 (2013).

[35] V. D. Ky, Planar Hall effect in ferromagnetic films, Phys. Status Solidi B **26**, 565 (1968).

[36] W. Limmer, M. Glunk, J. Daeubler, T. Hummel, W. Schoch, R. Sauer, C. Bihler, H. Huebl, M. S. Brandt, and S. T. B. Goennenwein, Angle-dependent magnetotransport in cubic and tetragonal ferromagnets: Application to (001)- and (113)*a*-oriented (Ga, Mn)As, Phys. Rev. B **74**, 205205 (2006).

[37] J. R. Lindemuth and B. C. Dodrill, Anomalous Hall effect magnetometry studies of magnetization processes of thin films, J. Magn. Magn. Mater. **272-276**, 2324 (2004).

[38] N. Nabben, G. Sala, U. Nowak, M. Krüger, and S. T. B. Goennenwein, Magnetization fluctuations and magnetic after-effect probed via the anomalous Hall effect, Phys. Rev. Res. **6**, 043283 (2024).

[39] J. X. Shen, R. D. Kirby, K. Wierman, Z.-S. Shan, D. J. Sellmyer, and T. Suzuki, Magnetization reversal and defects in Co/Pt multilayers, J. Appl. Phys **73**, 6418 (1993).

[40] See Supplemental Material at http://link.aps.org/supplemental/10.1103/PhysRevB.111.014441 for the magnetometry measurements, measurement of slow magnetic relaxation using SQUID, the dependence of the lock-in signals to the integration time and reference frequency as well as temperature-dependent measurements on MnAl.

[41] G. Bertotti, Energetic and thermodynamic aspects of hysteresis, Phys. Rev. Lett. **76**, 1739 (1996).

[42] G. Kloos, *Application of lock-in amplifiers in optics* (SPIE Press, Bellingham, WA, 2018).

[43] Zurich Instruments, Principles of lock-in detection and the state of the art (2023), https://www.zhinst.com/sites/default/files/documents/2023-04/zi_whitepaper_principles_of_lock-in_detection_0.pdf.

[44] M. S. Keshner, 1/f noise, Proc. IEEE **70**, 212 (1982).

[45] V. Radeka, 1/|f| Noise in physical measurements, IEEE Trans. Nucl. Sci. **16**, 17 (1969).

[46] N. Roschewsky, E. S. Walker, P. Gowtham, S. Muschinske, F. Hellman, S. R. Bank, and S. Salahuddin, Spin-orbit torque and Nernst effect in Bi-Sb/Co heterostructures, Phys. Rev. B **99**, 195103 (2019).

[47] C. O. Avci, K. Garello, M. Gabureac, A. Ghosh, A. Fuhrer, S. F. Alvarado, and P. Gambardella, Interplay of spin-orbit torque and thermoelectric effects in ferromagnet/normal-metal bilayers, Phys. Rev. B **90**, 224427 (2014).

[48] J. M. D. Coey, New permanent magnets; manganese compounds, J. Phys.: Condens. Matter **26**, 064211 (2014).

[49] F. Takata, T. Gushi, A. Anzai, K. Toko, and T. Suemasu, Structural characterization and magnetic properties of $L1_0$-MnAl films grown on different underlayers by molecular beam epitaxy, J. Cryst. Growth **486**, 19 (2018).

[50] M. Oogane, K. Watanabe, H. Saruyama, M. Hosoda, P. Shahnaz, M. Kurimoto, Y. Kubota, and Y. Ando, $L1_0$-ordered

MnAl thin films with high perpendicular magnetic anisotropy, Jpn. J. Appl. Phys. **56**, 0802A2 (2017).

[51] S. Mao, J. Lu, H. Wang, X. Zhao, X. Wei, and J. Zhao, Observation of tunneling magnetoresistance effect in $L1_0$-MnAl/MgO/Co_2MnSi/MnAl perpendicular magnetic tunnel junctions, J. Phys. D: Appl. Phys. **52**, 405002 (2019).

[52] J. Z. Wei, Z. G. Song, Y. B. Yang, S. Q. Liu, H. L. Du, J. Z. Han, D. Zhou, C. S. Wang, Y. C. Yang, A. Franz, D. Többens, and J. B. Yang, τ-MnAl with high coercivity and saturation magnetization, AIP Adv. **4**, 127113 (2014).

[53] Y. Jia, Y. Wu, S. Zhao, S. Zuo, K. P. Skokov, O. Gutfleisch, C. Jiang, and H. Xu, $L1_0$ rare-earth-free permanent magnets: The effects of twinning versus dislocations in Mn-Al magnets, Phys. Rev. Mater. **4**, 094402 (2020).

[54] Y. Jia, Y. Wu, Y. Xu, R. Zheng, S. Zhao, K. P. Skokov, F. Maccari, A. Aubert, O. Gutfleisch, J. Wang, H. Wang, J. Zou, and C. Yiang, Roadmap towards optimal magnetic properties in $L1_0$-MnAl permanent magnets, Acta Mater. **245**, 118654 (2023).

[55] A. S. Volegov, K.-H. Müller, F. Bittner, T. Mix, D. S. Neznakhin, E. A. Volegova, K. Nenkov, L. Schultz, and T. G. Woodcock, Magnetic viscosity of $L1_0$ structured Mn-Ga and Mn-Al alloys, J. Magn. Magn. Mater. **441**, 750 (2017).

[56] D. Scheffler, S. Beckert, H. Reichlova, T. G. Woodcock, S. T. B. Goennenwein, and A. Thomas, Anomalous Nernst effect in perpendicularly magnetised τ-MnAl thin films, AIP Adv. **13**, 125227 (2023).